Catheterization and Cardiovascular Interventions

WILEY

ORIGINAL ARTICLE - BASIC SCIENCE OPEN ACCESS

Difference Between Low-Speed and High-Speed Rotational Atherectomy Using Two Types of Guidewires

Akito Kawamura[1] | Keita Okayama[1] | Hiroaki Nohara[2] | Tomoaki Nakano[1] | Yasushi Sakata[1]

[1]Department of Cardiovascular Medicine, Osaka University Graduate School of Medicine, Osaka, Japan | [2]Division of Cardiology, Osaka Rosai Hospital, Osaka, Japan

Correspondence: Keita Okayama (okayama@cardiology.med.osaka-u.ac.jp)

Received: 20 November 2025 | **Revised:** 7 January 2026 | **Accepted:** 2 February 2026

Keywords: in vivo experimental study | optical coherence tomography | rotational atherectomy | severe calcified lesion

ABSTRACT

Background: Debulking devices are necessary to treat severe calcified lesions. Rotational atherectomy (RA) is widely employed to modify calcified plaques, but the influence of procedural variables, such as guidewire type and ablation speed, on ablation outcomes is not well established.

Aims: This study aimed to evaluate the effect of guidewire type and rotational speed on ablation performance during RA using an in vitro simulation system using HEARTROID system® and optical coherence tomography (OCT).

Methods: Using the HEARTROID® cardiac simulator, twenty calcified lesions in a mid-left anterior descending (LAD) artery model were ablated. Two types of RotaWire-floppy and extra-support-were tested at high (190,000 rpm) and low (140,000 rpm) speeds. Pre- and post-ablation OCT were performed to evaluate lumen area, directional discrepancy between pre-OCT or guidewire position and actual ablation direction, and the size of debulked regions.

Results: A total of 171 debulked cross-sections were analyzed. In floppy wire groups, high-speed RA was associated with significantly greater directional discrepancy compared to low-speed RA. Conversely, in extra-support wire groups, high-speed RA resulted in significantly smaller directional discrepancy than low-speed RA. Debulked area tended to be larger at low speed for floppy wire and at high speed for extra-support wire, though differences were not statistically significant. The combination of extra-support wire and high-speed ablation produced the most predictable and controlled debulking.

Conclusions: Guidewire type and rotational speed significantly influence directional control during RA. High-speed ablation with an extra-support wire minimizes directional discrepancy and may allow more predictable and controlled lesion modification.

1 | Introduction

Percutaneous coronary intervention (PCI) in patients with severe coronary artery calcification remains technically challenging, as it hinders device delivery and limits optimal stent expansion [1, 2]. To facilitate stent deployment and achieve adequate expansion, debulking devices such as rotational atherectomy (RA) and the orbital atherectomy system (OAS) are commonly employed for lesion modification in heavily calcified lesions [3]. In RA, two key variables that can be adjusted are the type of RotaWire (Boston Scientific, Marlborough, MA, USA) used and the rotational speed. In terms of rotational speed, previous studies have reported conflicting results regarding the size of the debulked area between low and high speed [4, 5]. Furthermore, limited data are available

Abbreviations: ANOVA, analysis of variance; LAD, left anterior descending; OAS, orbital atherectomy system; OCT, optical coherence tomography; PCI, percutaneous coronary intervention; RA, rotational atherectomy.

regarding the differences between the two types of RotaWire drive floppy and extra support. On the other hand, the HEARTROID® system (JMC, Yokohama, Japan), a pulsatile cardiac catheterization simulator with silicone three-dimensional printed heart model based on the human cardiac computed tomographic data, has recently been utilized for catheterization training under X-ray fluoroscopy and for catheter device evaluation. In both clinical cases and animal experiments, it is not feasible for us to perform the procedure in the same situation repeatedly. However, this system enables us to simulate conditions more closely resembling reality in an in vitro setting, as previously reported [6]. Moreover, we have already reported the differences of ablation style using orbital atherectomy system, optical coherence tomography and the HEARTROID in the previous study [7]. Therefore, this study aimed to evaluate the difference of the ablation style between low and high speed RA with in vitro simulation experiment using the two types of wire.

2 | Methods

2.1 | Experimental Protocols

The HEARTROID® system consists of three major components: a heart model, a plastic tank, and a pulsatile pump capable of generating heart rates ranging from 30 to 120 beats per minute (bpm). For this experiment, the heart rate was fixed at 60 bpm. The heart model employed in this study contains a pocket in the mid–left anterior descending (LAD) artery, into which three-dimensional (3D)-printed, calcification-mimicking disease models (hereafter referred to as calcification models) made of epoxy resin were inserted (Figure 1A,B). The LAD calcification model was designed with the following specifications: total length 20 mm, stenosis length 10 mm, minimum lumen diameter 1.4 mm, proximal reference diameter 4.0 mm, and distal reference diameter 2.7 mm, each with a bilateral tolerance of 0.05 mm under X-ray fluoroscopy. The model exhibited an angulation of 19.1 degrees. Details of the calcified model are shown in Figure 1C. A seven-French guide catheter, Mach1™ Q3.5 (Boston Scientific, Marlborough, MA, USA), was engaged in the left coronary artery. In the floppy wire group, a RotaWire drive floppy was advanced to the distal LAD, whereas in the extra-support wire group, a RotaWire drive extra-support was inserted. Pre-procedural optical coherence tomography (OCT) was performed using the Dragonfly OPTIS imaging catheter (Abbott Vascular, Santa Clara, CA, USA). To investigate the effect of guiding catheter position on wire orbit, the tip of the guiding catheter was adjusted. Two configurations were tested: shallow engagement and deep engagement. Significant differences were observed between these two configurations (Figure 2). After confirming the influence of guiding catheter position on wire orbit, the catheter was intentionally fixed in a deep engagement position for all subsequent experiments to isolate the effects of wire type and rotational speed. Following pre-OCT imaging, high-speed ablation (190,000 rpm) was performed using RA ($N = 10$) in both groups, followed by

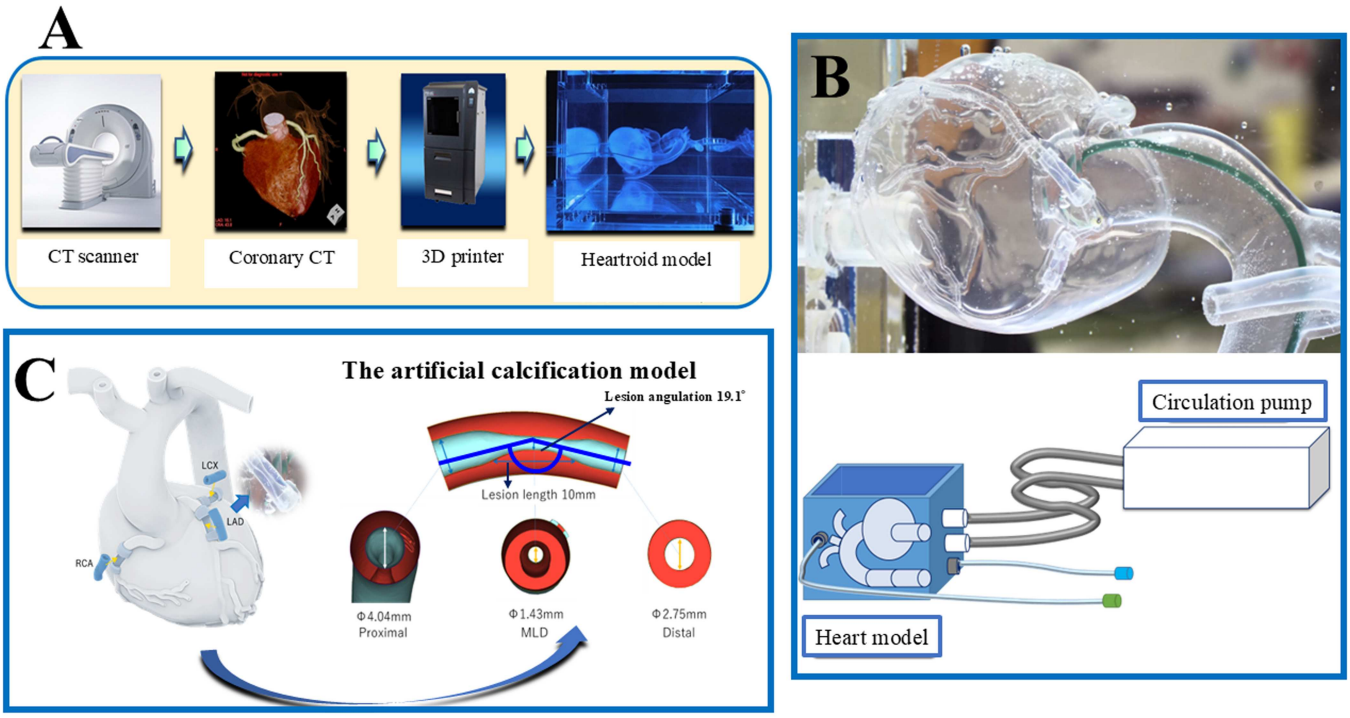

FIGURE 1 | The in vitro experimental system in this study. (A) This figure illustrates the manufacturing process of the Heartroid® system. The heart model was created by 3D printer in basis of the real human heart imaged by computed tomography scanner. (B) The heart model was connected to the circulation pump. This circulation pump plays a key role of the pulsatile heart model and enables simulation like the real percutaneous coronary intervention. (C) The calcification model was inserted into the mid of left anterior descending in the Heartroid® system. The calcification model was made of epoxy resin using the 3D printer. The model was the concentric type. Moreover, its length was 20 mm, while the lesion length was 10 mm. The diameter of the proximal, the distal and the lesion site were shown. [Color figure can be viewed at wileyonlinelibrary.com]

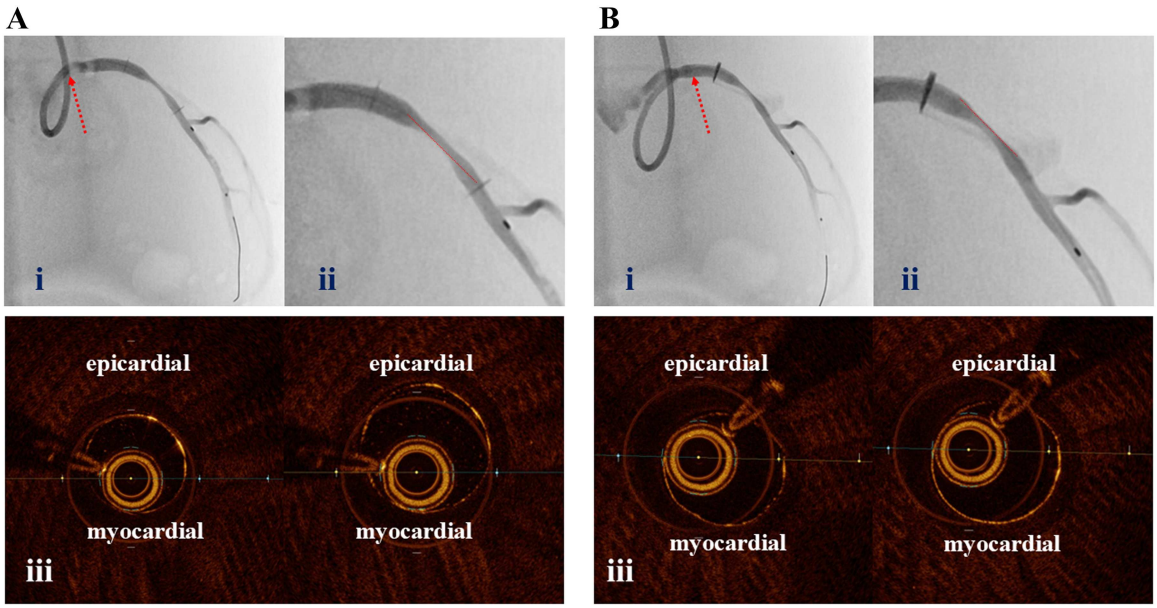

FIGURE 2 | Difference of wire orbit by the guiding catheter's position. (A) Shallow guiding position. (i) Angiography of shallow guiding position. The guiding catheter was inserted shallowly. The red arrow indicates the tip of the guiding catheter. (ii) Magnified image of angiography. The red line indicates the orbit of the wire. The guide wire passed inner side. (iii) OCT images showed wire and OCT catheter existed in myocardial area. (B) Deep guiding position. (i) Angiography of deep guiding position. The guiding catheter was inserted deeply. The red arrow indicates the tip of the guiding catheter. (ii) Magnified image of angiography. The red line indicates the orbit of the wire. The guide wire passed outer line. (iii) OCT images showed wire and OCT catheter existed relatively in epicardial area compared to those of shallow guiding catheter. [Color figure can be viewed at wileyonlinelibrary.com]

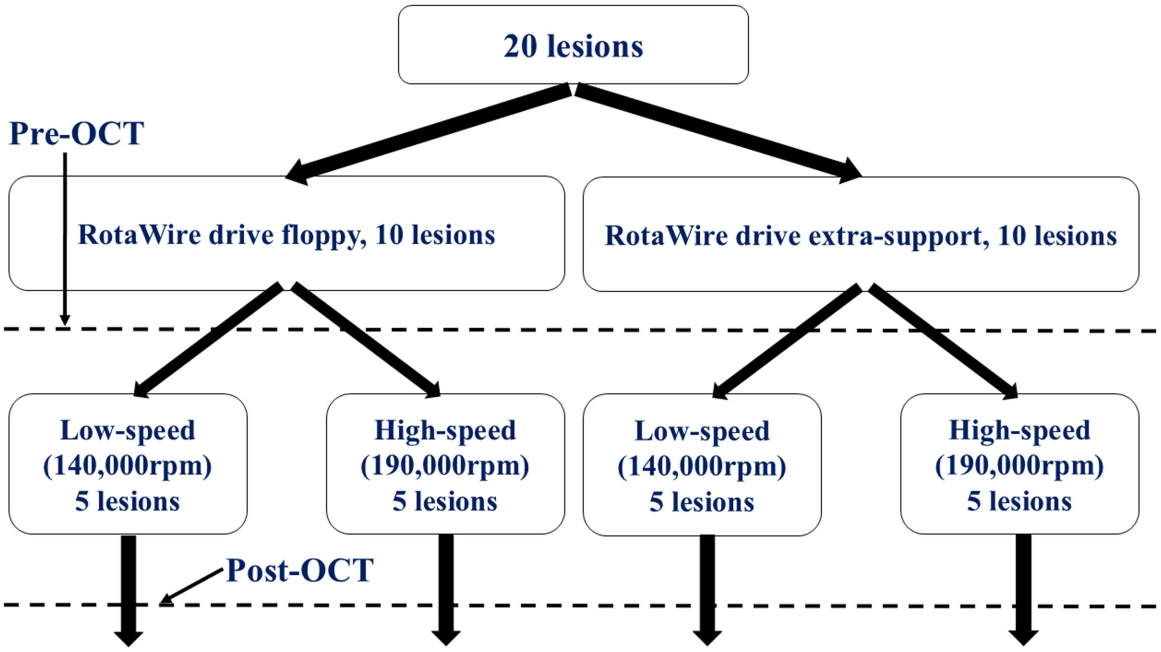

FIGURE 3 | Study flowchart. The floppy wire group included 10 lesions, the extra-support group also 10 lesions. Low-speed and high-speed ablation were performed in each group. OCT = optical coherence tomography. [Color figure can be viewed at wileyonlinelibrary.com]

low-speed ablation (140,000 rpm; $N = 10$). A 1.75 mm Rota burr was selected for the experiment, with precautions taken to prevent a drop in rotational speed exceeding 5000 rpm and to limit each run to a maximum of 20 s. The burr platform was positioned proximal to the lesion, ensuring preservation of distal flow. From this platform, the burr was advanced slowly toward the lesion and then deliberately withdrawn back to the platform in a controlled manner. Burr manipulation was performed at a slow and steady speed, avoiding a pecking motion. This advance-and-withdraw maneuver was repeated three times during a single ablation session. Post-ablation OCT images were obtained after the burr had passed through the lesion (Figure 3). In this study, polishing runs were intentionally not performed. All procedures were performed by a single experienced operator

who was aware of the wire type and rotational speed, as these are inherent procedural parameters during RA; however, the specific study hypotheses, including the expected interaction between wire type and rotational speed, were not disclosed. Predefined procedural rules regarding burr advancement technique, run duration, and acceptable RPM reduction were strictly followed. In each case, the calcification model was changed to a new one when the burr passed the lesion. These methods were similar to the previous study [7].

2.2 | OCT Analysis

Quantitative and qualitative OCT analyses were performed using dedicated software (Off-line Review Software, version E.0.2; Abbott Vascular, Santa Clara, CA, USA). For both pre-procedural and post-procedural OCT images, all cross-sectional images were initially screened for quality assessment and excluded from analysis if image quality was deemed insufficient due to artifacts or reverberation [8]. Quantitative and qualitative measurements were performed on every 1-mm frame along the 20-mm-long calcification lesion model. Consequently, each case included 21 analyzed cross-sections, and only the debulked cross-sections were included in the analysis for this study.

In the pre-procedural OCT analysis, the lumen contour was manually traced in each analyzed frame, and the lumen area was measured. Subsequently, the center of the lumen and the center of the guidewire were identified. The following distances were measured in all analyzed cross-sections of the pre-procedural OCT images: (i) between the guidewire and the nearest vessel wall and (ii) between the OCT catheter and the nearest vessel wall (Figure 4A).

Each OCT cross section was divided into four quadrants around the center of the lumen rotating the branch of the diagonal toward nine o'clock. Spatial orientation in the vessel wall was as follows: epicardial quadrant, myocardial quadrant and lateral quadrants. In addition, lateral quadrants were divided into right lateral and left lateral quadrants. The positions of the center of the guidewire and the OCT catheter were divided into one of four quadrants (Figure 4B,C). Serial pre- and post-procedural OCT images were carefully reviewed side by side, and the analyzed cross-sections were matched based on their distance from landmarks such as side branches or the site of the calcification model. A cross-section was considered to contain a debulked region if the lumen area increased by more than 5% after RA ablation and if the region exhibiting lumen enlargement showed distinct traces of burr debulking on the post-RA OCT image. In cross-sections containing debulked regions, the distribution of the center of the guidewire, OCT catheter, and debulked region within the quadrant of the merged OCT image was analyzed. Directional differences among the pre-OCT lumen, pre-wire position, and the actual debulked area were qualitatively assessed using angular measurements. The debulked area was calculated as the post-RA lumen area minus the pre-RA lumen area. Additionally, the width and depth of the debulked area were measured manually (Figure 4D) [7].

2.3 | Statistical Analysis

All statistical analyses were performed using JMP version 18 software (SAS Institute Inc., Cary, North Carolina, USA) and the statistical significance was assessed at a p-level of 0.05. The continuous variables are expressed as the mean ± SD or median (interquartile range) and categorical variables as the count (percentage). For the continuous variables, the difference between the two groups were made with the nonparametric Mann-Whitney U test, and the categorical variables were compared with a Fisher exact test at the lesion level. All variables were analyzed at the lesion level. The pre-procedural and post -procedural parameters were compared in all lesions.

Among four groups, the specific post-procedural parameters were compared in a one-way analysis of variance (ANOVA). If a significant overall difference was found, post hoc pairwise comparisons were conducted between four groups using Dunnett's test.

3 | Results

3.1 | Procedural Characteristics

Procedural characteristics related to burr manipulation across the four experimental groups are summarized in Table 1. All individual ablation runs in each group were limited to less than 20 s, and the maximum rotational speed reduction did not exceed 10,000 rpm. Overall, the number of burr runs, ablation time, and rotational speed reduction were comparable among

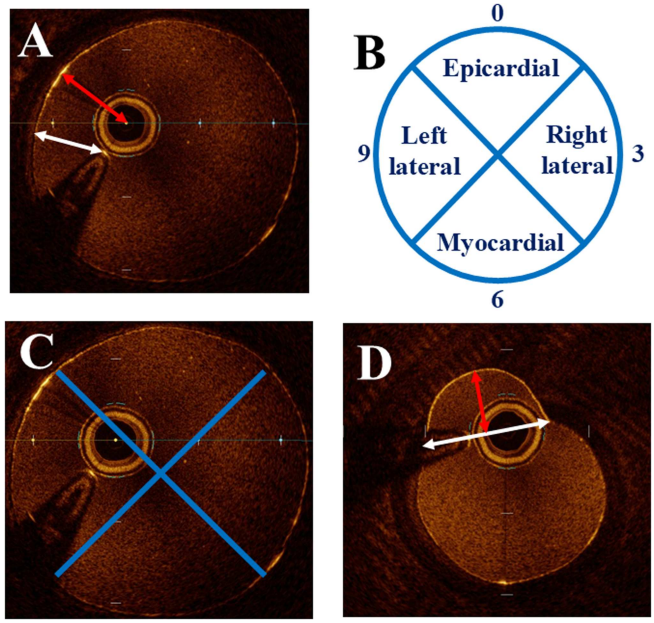

FIGURE 4 | Measurement of OCT image. (A) The distance between the guidewire and the nearest vessel wall (white arrow) and the distance between the OCT catheter and the nearest vessel wall (red arrow) were shown. (B) Spatial orientation of each OCT cross-section were categorized as myocardial, epicardial, left lateral of right lateral quadrants around the center of the lumen. The positions of the center of the guidewire and OCT catheter were assessed in each cross-section. (C) In this image, the positions of OCT catheter and guidewire were categorized as left lateral. (D) A post OCT image. The direction of debulked area was at the epicardial quadrant. The depth of the debulked area (red arrow) and the width of the debulked area (white arrow) were shown. OCT, optical coherence tomography. [Color figure can be viewed at wileyonlinelibrary.com]

TABLE 1 | Procedural characteristics across the four groups.

	FL group ($N = 5$)	FH group ($N = 5$)	SL group ($N = 5$)	SH group ($N = 5$)
Number of burr runs, n	9.0 (9.0–10.0)	8.0 (6.5–8.5)	9.0 (7.5–9.5)	6.0 (5.0–7.0)
Mean ablation time, s	7.8 (7.2–8.7)	7.3 (6.9–7.6)	6.8 (6.3–7.1)	7.2 (6.7–7.4)
Total ablation time, s	70 (65–87)	56 (50–60)	58 (52–63)	41 (35–52)
Maximum RPM reduction, rpm	9000 (7000–9000)	5000 (4500–7000)	8000 (6500–8500)	6000 (3500–6000)

Abbreviations: FH, floppy high-speed; FL, floppy low-speed; rpm, rotations per minute; SH, extra-support high-speed; SL, extra-support low-speed.

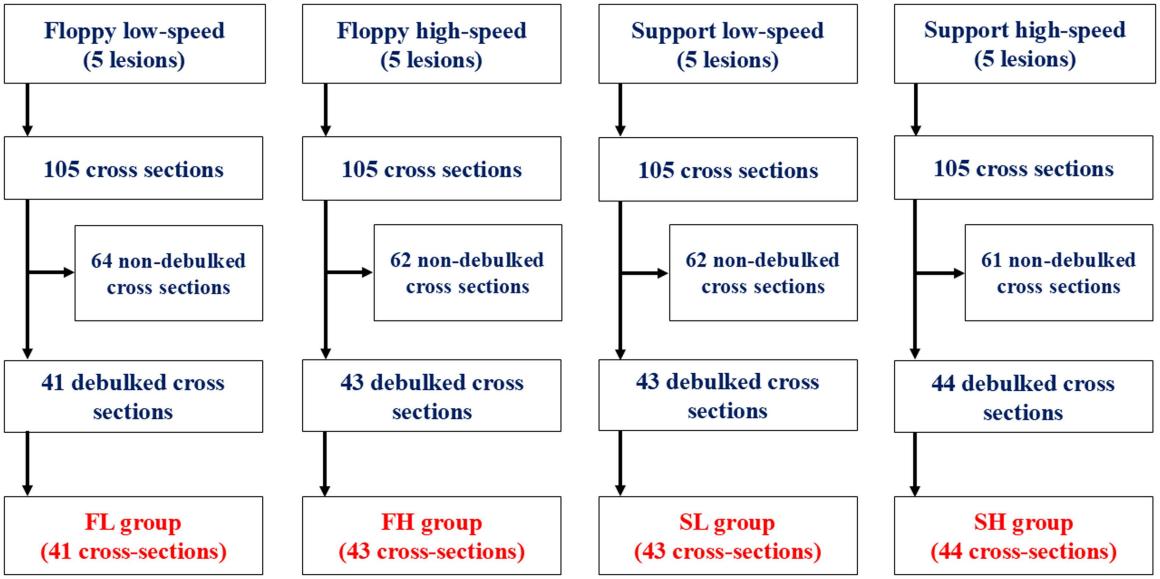

FIGURE 5 | Flow chart of cross-sectional evaluation of OCT after rota burr passage. After ablation, floppy low-speed (FL group) had 41 cross-sections, floppy high-speed (FH group) 43 cross-sections, support low-speed (SL group) 43 cross-sections, and support high-speed (SH group) 44 cross-sections. OCT, optical coherence tomography. [Color figure can be viewed at wileyonlinelibrary.com]

the groups, indicating that a standardized ablation protocol was applied.

3.2 | Cross-Section Level OCT Analysis

A total of 420 coronary cross-sections were obtained from 20 calcified lesions: five in the floppy wire with low-speed (140,000 rpm) group (FL), five in the floppy wire with high-speed (190,000 rpm) group (FH), five in the extra-support with low-speed (140,000 rpm) group (SL), and five in the extra-support with high-speed (190,000 rpm) group (SH). Of these, 249 non-debulked cross-sections were excluded, leaving 171 debulked cross-sections for analysis (41 from FL, 43 from FH, 43 from SL, and 44 from SH) (Figure 5).

3.3 | Comparison Between High and Low Speed Ablation Using Two Types of Wire

In the floppy wire groups, pre-OCT analysis revealed no significant differences in lumen area, the distance between the OCT catheter and the vessel wall, or the distance from the OCT catheter to the guidewire between the FL and FH groups (Table 2). Post-OCT analysis also showed no significant differences in debulked areas between the two groups, whereas the discrepancy between the pre-OCT catheter direction and the actual debulked direction was significantly greater in the FH group than in the FL group (Table 3).

In the support wire groups, no significant differences were observed in pre-OCT parameters between the SL and SH groups (Table 4). However, the directional discrepancy between the pre-wire or OCT catheter and the actual ablation direction was significantly greater in the SL group compared with the SH group (Table 5).

3.4 | ANOVA and Dunnett's Test for Debulking Parameters Among Four Groups

A one-way ANOVA was performed to compare the debulked area, the directional discrepancy between the pre-wire position and the actual ablation direction, and the directional discrepancy between the pre-OCT catheter position and the actual ablation direction among the four groups. All three parameters showed statistically significant differences ($p = 0.006$, $p < 0.001$, and $p < 0.001$, respectively). Given these overall effects, Dunnett's post hoc test was applied, demonstrating that both parameters related to predictable debulking bias were lowest in the SH group compared with the other groups (Figure 6A–C). The actual ablation directions, classified by quadrants, are shown in Figure 6D, and representative images are provided in Figure 7.

TABLE 2 | Comparison of pre-OCT image between FL and FH group.

	FL group ($N = 41$)	FH group ($N = 43$)	p value
Lumen area, mm^2	2.04 (1.69–3.04)	2.14 (1.68–3.05)	0.904
Mean diameter, mm	1.61 (1.46–1.97)	1.66 (1.46–1.98)	1.000
Distance between the guidewire and the vessel wall, mm	0.23 (0.15–0.42)	0.23 (0.17–0.37)	0.744
Distance between the OCT catheter and the vessel wall, mm	0.44 (0.40–0.52)	0.44 (0.42–0.57)	0.407
Guidewire position (four quadrants)			
Epicardium	6 (14.6)	2 (4.7)	
Left lateral	29 (70.7)	31 (72.1)	
Right lateral	0 (0)	0 (0)	
Myocardium	6 (14.6)	10 (23.3)	
OCT catheter position (four quadrants)			
Epicardium	17 (41.5)	16 (37.2)	
Left lateral	24 (58.5)	25 (58.1)	
Right lateral	0 (0)	0 (0)	
Myocardium	0 (0)	2 (4.7)	

Note: Abbreviations are the same as in Table 1.
Abbreviation: OCT, optical coherence tomography.

TABLE 3 | Comparison of post-OCT image between FL and FH group.

	FL group ($N = 41$)	FH group ($N = 43$)	p value
Lumen area, mm^2	3.25 (2.75–4.28)	3.20 (2.52–4.29)	0.327
Debulked area, mm^2	1.09 (0.83–1.40)	0.95 (0.76–1.24)	0.100
The width of debulked area, mm	1.71 (1.63–1.78)	1.64 (1.57–1.72)	0.018
The depth of debulked area, mm	0.52 (0.38–0.63)	0.42 (0.32–0.58)	0.246
The direction of debulked area (four quadrants)			
Epicardium	32 (78.1)	43 (100)	
Left lateral	9 (21.9)	0 (0)	
Right lateral	0 (0)	0 (0)	
Myocardium	0 (0)	0 (0)	
Directional discrepancy between the pre-wire position and the actual ablation direction (degrees)	90 (60–90)	90 (90–90)	0.023
Directional discrepancy between the pre-OCT catheter position and the actual ablation direction (degrees)	60 (30–60)	90 (60–120)	0.002

Note: Abbreviations are the same as in Table 1.
Abbreviation: OCT, optical coherence tomography.

4 | Discussion

The main findings of this study were as follows: (i) the orbit of the wire was influenced by the position and configuration of the guiding catheter; (ii) in the floppy wire groups, high-speed (190,000 rpm) atherectomy was associated with a significantly greater directional discrepancy compared with low-speed (140,000 rpm) ablation; (iii) conversely, in the extra-support wire groups, high-speed (190,000 rpm) atherectomy resulted in a significantly smaller directional discrepancy than low-speed (140,000 rpm) ablation; and (iv) the combination of an extra-support wire and high rotational speed yielded the smallest directional discrepancy among all four groups.

Although drug-eluting stents dramatically reduce the incidence of angiographic restenosis and the need for repeat revascularization, optimal stent deployment is essential to achieve favorable clinical outcomes [9]. Previous studies have shown that severely calcified coronary artery lesions often lead to stent underexpansion, failed stent delivery, and damage to the stent polymer during PCI [2, 10, 11]. To overcome these technical challenges, ablation devices such as rotational atherectomy (RA) and orbital atherectomy systems (OAS) have been used to modify severely calcified plaques. When using RA, operators can choose among several variables, such as the type of guidewire and the ablation speed. However, few studies have investigated the effects of these factors. Understanding these differences is important for safe ablation, as RA can sometimes cause relatively severe complications [12].

In this study, we first demonstrated that wire bias is easily influenced by the condition of the guiding catheter. If wire bias varies due to guide catheter migration, accurate assessment of ablation outcomes becomes difficult. For example, if pre-OCT

TABLE 4 | Comparison of pre-OCT image between SL and SH group.

	SL group ($N = 43$)	SH group ($N = 44$)	p value
Lumen area, mm^2	2.06 (1.71–3.09)	1.98 (1.66–3.01)	0.656
Mean diameter, mm	1.60 (1.48–2.00)	1.59 (1.45–1.97)	0.677
Distance between the guidewire and the vessel wall, mm	0.30 (0.22–0.44)	0.25 (0.21–0.33)	0.339
Distance between the OCT catheter and the vessel wall, mm	0.44 (0.42–0.56)	0.48 (0.43–0.57)	0.150
Guidewire position (four quadrants)			
Epicardium	12 (27.9)	19 (43.2)	
Left lateral	7 (16.3)	19 (43.2)	
Right lateral	0 (0)	0 (0)	
Myocardium	24 (55.8)	6 (13.6)	
OCT catheter position (four quadrants)			
Epicardium	4 (9.3)	13 (29.6)	
Left lateral	39 (90.7)	31 (70.5)	
Right lateral	0 (0)	0 (0)	
Myocardium	0 (0)	0 (0)	

Note: Abbreviations are the same as in Table 1.
Abbreviation: OCT, optical coherence tomography.

TABLE 5 | Comparison of post-OCT image between SL and SH group.

	SL group ($N = 43$)	SH group ($N = 44$)	p value
Lumen area, mm^2	3.04 (2.61–3.86)	3.23 (2.77–4.14)	0.177
Debulked area, mm^2	0.89 (0.67–1.11)	1.19 (0.84–1.33)	0.002
The width of debulked area, mm	1.67 (1.61–1.72)	1.70 (1.66–1.76)	0.087
The depth of debulked area, mm	0.38 (0.32–0.52)	0.49 (0.38–0.63)	0.011
The direction of debulked area (four quadrants)			
Epicardium	14 (32.6)	18 (40.9)	
Left lateral	29 (67.4)	26 (59.1)	
Right lateral	0 (0)	0 (0)	
Myocardium	0 (0)	0 (0)	
Directional discrepancy between the pre-wire position and the actual ablation direction (degrees)	60 (30–120)	45 (30–60)	0.014
Directional discrepancy between the pre-OCT catheter position and the actual ablation direction (degrees)	30 (15–45)	15 (0–30)	0.001

Note: Abbreviations are the same as in Table 1.
Abbreviation: OCT, optical coherence tomography.

imaging is performed with the guiding catheter in a shallow position, but RA is conducted with the catheter in a deeper position, parameters such as the directional discrepancy between pre-OCT catheter position and actual ablation direction may become inaccurate. In our experiment, the guiding catheter was consistently locked in a deep position, allowing us to collect highly precise data.

By analyzing pre- and post-debulking OCT images, we found that in the floppy wire setting, low-speed (140,000 rpm) ablation tended to produce a larger debulked area than high-speed (190,000 rpm) ablation, although the difference was not statistically significant. Conversely, in the extra-support wire setting, high-speed (190,000 rpm) ablation tended to achieve a larger debulked area. This may explain the controversial findings in previous studies regarding the relationship between ablation speed and debulked area.

Regarding directional discrepancy between the pre-wire or OCT catheter and the actual debulked orientation, high-speed (190,000 rpm) ablation was associated with greater discrepancies in the floppy wire group. In contrast, in the extra-support wire group, the opposite pattern was observed. Notably, across all four groups, ablation performed with an extra-support wire at high speed (190,000 rpm) was associated with the smallest directional discrepancy, strongly supporting intentional debulking. From a clinical perspective, minimizing wire bias and directional discrepancy is crucial, as excessive deviation may increase the risk of vessel wall injury or perforation, which causes poor clinical outcome [13]. Our results suggest that using

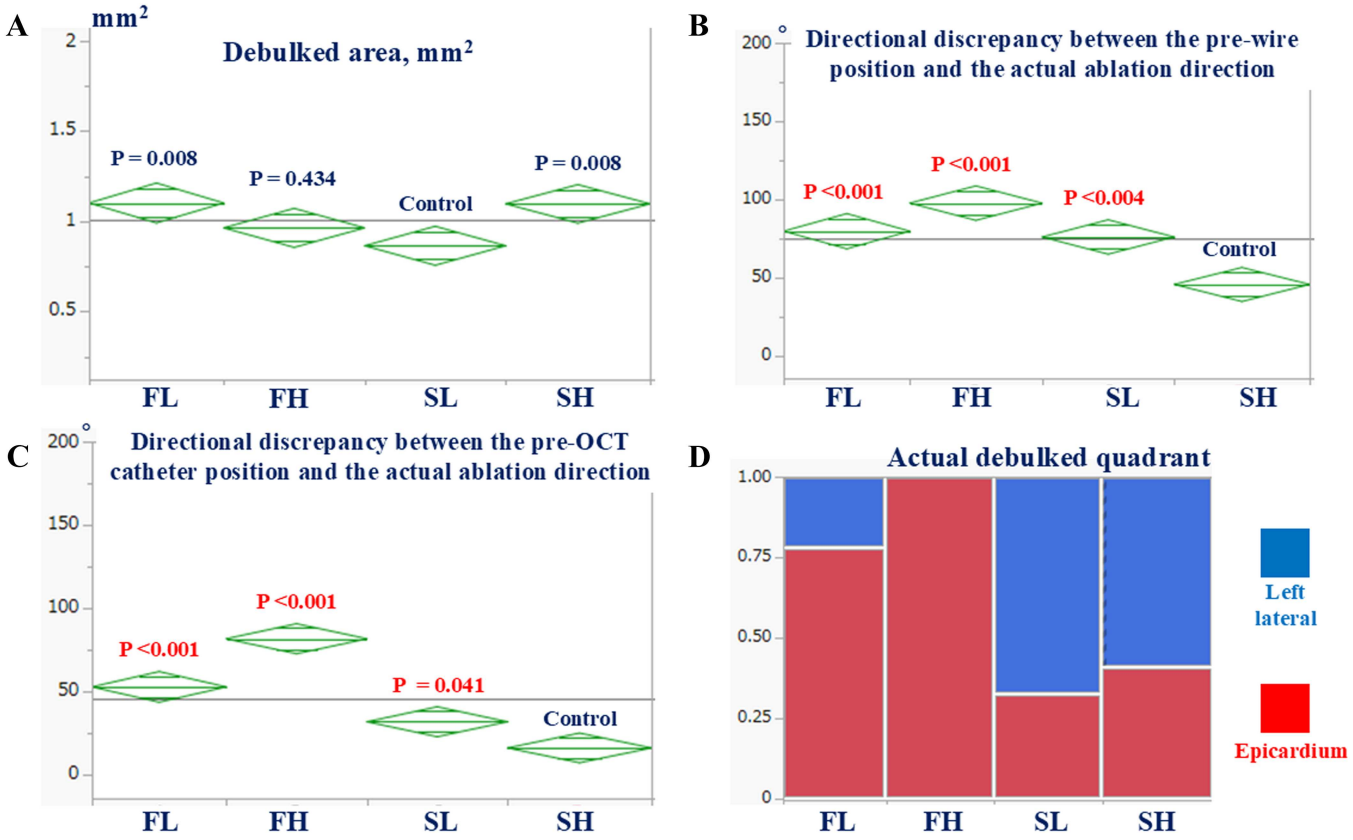

FIGURE 6 | Comparison of the post-OCT parameters between the four groups. The extra-support high-speed group demonstrated the smallest directional discrepancy among all four groups. OCT = optical coherence tomography, FL, floppy low-speed; FH, floppy high-speed; SL, support low-speed; SH, support high-speed. [Color figure can be viewed at wileyonlinelibrary.com]

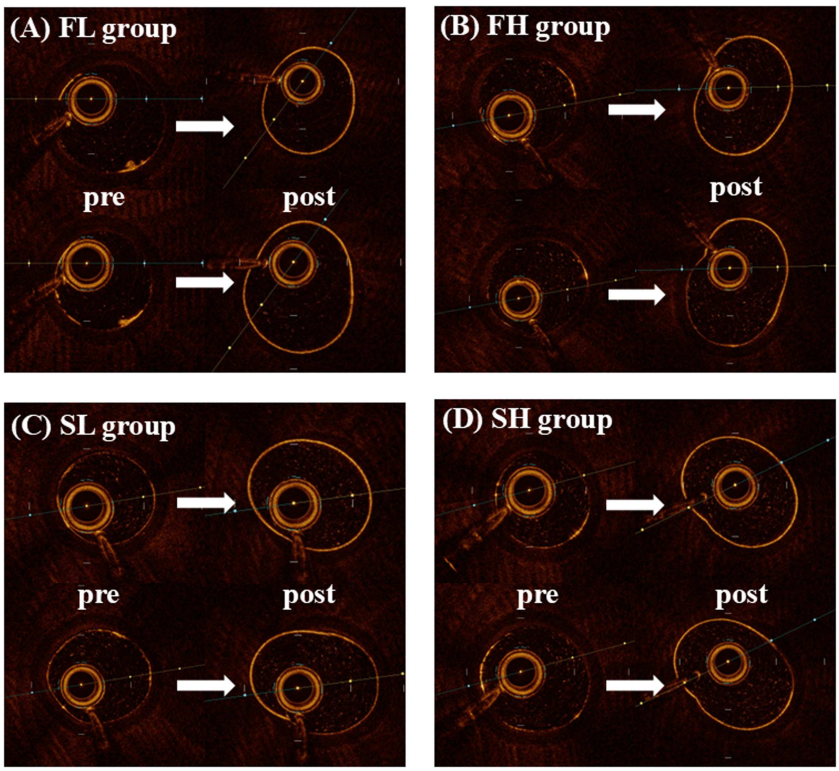

FIGURE 7 | The representative pre- and post-procedural OCT images. Representative pre- and post-ablation OCT images from the four experimental groups are shown. Post-ablation OCT images in the extra-support high-speed (SH) group demonstrate the smallest directional discrepancy. OCT = optical coherence tomography, FL, floppy low-speed; FH, floppy high-speed; SL, support low-speed; SH, support high-speed. [Color figure can be viewed at wileyonlinelibrary.com]

an extra-support wire at high-speed (190,000 rpm) may provide more predictable and controlled ablation.

In terms of wire selection, Figure 6D demonstrated unexpected results: the epicardium was more frequently debulked in the floppy wire group, regardless of the debulking speed of RA. One possible explanation is that, compared with the extra-support wire, the actual ablation direction with the floppy wire may be more likely to shift toward the epicardial region. Uncontrolled epicardial debulking can lead to severe complications, as epicardial rupture is typically associated with cardiac tamponade [14].

These findings also indicate that performing OCT imaging prior to RA may reduce the risk of severe complications such as coronary artery perforation or dissection. When an eccentric calcified plaque is present and there is little tolerance for directional deviation, high-speed (190,000 rpm) ablation using an extra-support wire may be preferable. Therefore, interventional cardiologists performing RA should be well-informed about how wire type and rotational speed influence ablation outcomes.

4.1 | Limitations of the Study

Several limitations should be acknowledged. First, the study was performed in an in vitro simulation setting using the HEARTROID® system, which does not fully replicate the complexities of in vivo coronary physiology such as vessel compliance, blood flow, and hemodynamic interactions. Direct conclusions regarding clinical safety cannot be drawn from this experimental model alone. Second, the number of analyzed lesions was limited, and clinical outcomes were not assessed. Third, OCT-based evaluation, while detailed, may have technical limitations in precisely reflecting the true ablation geometry. Further studies with larger sample sizes, in vivo validation, and long-term clinical follow-up are warranted to confirm the clinical applicability of these findings.

5 | Conclusions

In conclusion, this in vitro study demonstrates that high-speed (190,000 rpm) rotational atherectomy using an extra-support wire minimizes directional discrepancy and may allow more predictable and controlled lesion modification in calcified lesions.

Conflicts of Interest

The authors declare no conflicts of interest.

References

1. M. S. Lee and N. Shah, "The Impact and Pathophysiologic Consequences of Coronary Artery Calcium Deposition in Percutaneous Coronary Interventions," *Journal of Invasive Cardiology* 28, no. 4 (2016): 160–167.

2. M. Abdel-Wahab, G. Richardt, H. Joachim Büttner, et al., "High-Speed Rotational Atherectomy Before Paclitaxel-Eluting Stent Implantation in Complex Calcified Coronary Lesions," *JACC. Cardiovascular Interventions* 6, no. 1 (2013): 10–19, https://doi.org/10.1016/j.jcin.2012.07.017.

3. M. V. Madhavan, M. Tarigopula, G. S. Mintz, A. Maehara, G. W. Stone, and P. Généreux, "Coronary Artery Calcification," *Journal of the American College of Cardiology* 63, no. 17 (2014): 1703–1714, https://doi.org/10.1016/j.jacc.2014.01.017.

4. N. Kobayashi, M. Yamawaki, K. Hirano, et al., "Additional Debulking Efficacy of Low-Speed Rotational Atherectomy After High-Speed Rotational Atherectomy for Calcified Coronary Lesion," *International Journal of Cardiovascular Imaging* 36, no. 10 (2020): 1811–1819, https://doi.org/10.1007/s10554-020-01912-7.

5. T. Yamamoto, S. Yada, Y. Matsuda, et al., "A Novel Rotablator Technique (Low-Speed Following High-Speed Rotational Atherectomy) Can Achieve Larger Lumen Gain: Evaluation Using Optimal Frequency Domain Imaging," *Journal of Interventional Cardiology* 2019 (2019): 9282876, https://doi.org/10.1155/2019/9282876.

6. Y. Nishimoto, K. Okayama, M. Toma, and Y. Sato, "Different Positions of the Impella Device Between the Axillary and Femoral Approaches," *Circulation Reports* 4, no. 4 (2022): 183–184, https://doi.org/10.1253/circrep.CR-21-0164.

7. A. Kawamura, Y. Egami, N. Okamoto, et al., "Difference Between Antegrade and Retrograde Orbital Atherectomy System Debulking Using an Artificial Pulsatile Heart Model," *Catheterization and Cardiovascular Interventions: Official Journal of the Society for Cardiac Angiography & Interventions* 103, no. 1 (2024): 42–50, https://doi.org/10.1002/ccd.30925.

8. G. Guagliumi, K. Shimamura, V. Sirbu, et al., "Temporal Course of Vascular Healing and Neoatherosclerosis After Implantation of Durable- or Biodegradable-Polymer Drug-Eluting Stents," *European Heart Journal* 39, no. 26 (2018): 2448–2456, https://doi.org/10.1093/eurheartj/ehy273.

9. S. J. Hong, B. K. Kim, D. H. Shin, et al., "Effect of Intravascular Ultrasound-Guided vs Angiography-Guided Everolimus-Eluting Stent Implantation: The IVUS-XPL Randomized Clinical Trial," *Journal of the American Medical Association* 314, no. 20 (2015): 2155–2163, https://doi.org/10.1001/jama.2015.15454.

10. Y. Kobayashi, H. Okura, T. Kume, et al., "Impact of Target Lesion Coronary Calcification on Stent Expansion," *Circulation Journal* 78, no. 9 (2014): 2209–2214, https://doi.org/10.1253/circj.cj-14-0108.

11. M. Wiemer, T. Butz, W. Schmidt, K. P. Schmitz, D. Horstkotte, and C. Langer, "Scanning Electron Microscopic Analysis of Different Drug Eluting Stents After Failed Implantation: From Nearly Undamaged to Major Damaged Polymers," *Catheterization and Cardiovascular Interventions: Official Journal of the Society for Cardiac Angiography & Interventions* 75, no. 6 (2010): 905–911, https://doi.org/10.1002/ccd.22347.

12. K. Sakakura, Y. Ito, Y. Shibata, et al., "Clinical Expert Consensus Document on Rotational Atherectomy From the Japanese Association of Cardiovascular Intervention and Therapeutics: Update 2023," *Cardiovascular Intervention and Therapeutics* 38, no. 2 (2023): 141–162, https://doi.org/10.1007/s12928-022-00906-7.

13. K. Sakakura, T. Inohara, S. Kohsaka, et al., "Incidence and Determinants of Complications in Rotational Atherectomy: Insights From the National Clinical Data (J-PCI Registry)," *Circulation: Cardiovascular Interventions* 9, no. 11 (2016): e004278, https://doi.org/10.1161/circinterventions.116.004278.

14. A. Kawamura, Y. Egami, M. Nishino, and J. Tanouchi, "The C-CAT Sign May Predict Coronary Artery Perforation in Severe Calcified Lesions During Coronary Intervention: A Case Series," *European Heart Journal. Case Reports* 7, no. 3 (2023): ytad075, https://doi.org/10.1093/ehjcr/ytad075.